Crisis dynamics of a class of single-degree-of-freedom piecewise linear oscillators

Han Su[a], Yuan Yue[a,*], Run Liu[a], Celso Grebogi[b]

[a]*Applied Mechanics and Structure Safety Key Laboratory of Sichuan Province, School of Mechanics and Aerospace Engineering, Southwest Jiaotong University, Chengdu 610031, China*

[b]*Institute for Complex Systems and Mathematical Biology King's College, University of Aberdeen, Aberdeen AB24 3UE, United Kingdom*

Abstract: We investigate boundary crises, interior crises, and merging crises of a class of single-degree-of-freedom piecewise linear oscillators. From the perspective of the tangency of manifolds, the mechanisms of boundary crises are revealed, and the critical exponents are determined to distinguish between homoclinic crises and heteroclinic crises. As the parameter changes continuously, a chaotic orbit suddenly disappear at a certain critical point and reappear suddenly at another critical point. This phenomenon of two sudden changes in the chaotic orbit is related to boundary crises caused by the tangency of the stable and unstable manifolds of the same unstable periodic orbit. We call the regions formed by the intersection of the stable and unstable manifolds of the unstable period orbits associated with boundary crises as the escape regions. The change in the area of the escape regions induces the sudden disappearance and reappearance of a chaotic orbit. Detailed numerical simulations and analyses show that boundary crises may interact with the hysteresis loop, which induces complex dynamical behaviors, including transitions between a stable periodic orbit and a chaotic orbit repeatedly. In the two parameters space, changing a parameter value in the same direction will cause the decreases of the distance between the two boundary-crisis curves. When the distance is zero, there exist a coalescence point, which we call the crisis-disappearance point. Beyond this point, the chaotic orbit will no longer contact unstable periodic orbits, leading to the disappearance of the boundary crisis. Besides, the crisis-disappearance points associated with interior crises and merging crises are also uncovered.

Keywords：Single-degree-of-freedom piecewise linear oscillators；Chaotic orbits；Crises；Manifolds；Hysteresis.

---

[*] Correspondencing author.

E- mail addresses: suhan001116@163.com (Han Su), leyuan2003@sina.com (Yuan Yue), run139315@163.com (Run Liu), grebogi@adbn.ac.uk (Celso Grebogi).

1. Introduction

Many dynamical systems in practical engineering can be simulated as piecewise linear systems. Piecewise linear systems are an important research topic in the field of dynamical systems. Current research on the dynamics of piecewise linear systems includes modal response[1], stability analysis[2], grazing bifurcations[3], chaos control[4], and so on. Numerous numerical methods have been employed to analyze the time-frequency response of piecewise linear systems. Afzali et al.[5] used the multiple scales method to study secondary resonances of the van der Pol equation with parametric damping under both with and without external excitation. Jayaprakash et al.[6] proposed an averaging method applicable to a class of resonantly forced piecewise linear systems with zero offset. The harmonic balance method is one of the effective methods for analyzing amplitude-frequency responses and can be applied to piecewise linear systems[7] and quasi-periodically forced systems[8].

In their seminal work, Grebogi et al.[9][10] revealed crises in dynamical system, and elucidated the dynamical mechanism of crises. In dynamical systems, the sudden discontinuous changes in chaotic orbits are often related to crises. Crises occur when chaotic orbits collide with unstable periodic orbits. Based on the characteristic behavior of chaotic orbits after crises, they classified crises into boundary crises, interior crises, and merging crises.

Researchers have observed crises in a wide range of dynamical systems and experiments, and uncovered some new mechanisms that lead to the occurrence of crises. Yang et al.[11] considered a logistic map model driven by parametric noise and discovered a new crisis resulting from the formation of channels caused by the backward tangent bifurcation. Combining experimental data and employing symbolic dynamics techniques, Finardi et al.[12] obtained a precise criterion for interior crises by analyzing the symbolic sequence changes of unstable periodic orbits before and after heteroclinic crises. Hong and Xu[13] used the generalized cell mapping digraph (GCDM) method to study the crisis dynamics phenomenon of chaotic saddle colliding with chaotic orbits in a forced Duffing oscillator, referred to as chaotic crises. Tanaka et al.[14] considered a hybrid dynamical model obtained in a drug treatment system and discovered crises induced by grazing bifurcations. Liu et al.[15] investigated the phenomena of interior crises and boundary crises in fractional-order piecewise systems.

To achieve a deeper understanding of the crisis behavior, one must analyze manifolds[16][17]. When a boundary crisis occurs, the unstable periodic orbit colliding with the chaotic orbit is located on the basin boundary of the chaotic orbit, and its stable manifold forms the basin boundary of the chaotic orbit. During the crisis, its stable manifold becomes tangent to the branch of the unstable manifold toward the interior of the basin of attraction, and the chaotic orbit is the closure of this unstable manifold branch. The tangency of stable and unstable manifolds of the unstable periodic orbits on the basin boundary will also lead to basin boundary metamorphoses[18][19]. For interior crises or merging crises, the unstable periodic orbit that collides with the chaotic orbit is located within the basin of attraction. When the stable manifold becomes tangent to the unstable manifold, n-piece chaotic orbits are equal to the closure of the unstable manifold. Taking a quasi-periodically forced Hénon map as an example, Osinga and Feudel[20] found that the collision between chaotic orbits and unstable invariant circles can also lead to the occurrence of crises, and the two-dimensional stable manifold of the invariant circle becomes tangent to its own unstable manifold for crises.

Extending the boundary-crisis curve in the two-parameter space, each point on the curve is related to the tangency between stable and unstable manifolds of unstable periodic orbits. The intersection of boundary-crisis curves corresponding to two different unstable orbits results in a vertex, which is referred to as a double-crisis vertex[21][22]. As one continues the extension of the two curves through this vertex, the tangency of manifolds leads to interior crises and basin boundary metamorphoses. Initially, the boundary-crisis curve was thought to be piecewise smooth when the double-crisis vertex was discovered. However, subsequent research revealed that there are infinite small gaps along the boundary-crisis curve. These gaps are related to the existence of periodic windows in the chaotic region of the single-parameter bifurcation diagram[23]. In non-smooth systems, due to the occurrence of certain boundary crises related to grazing bifurcations[24], Mason and Piiroinen[25] discovered a new double-crisis vertex associated with the sudden disappearance of chaotic orbits. This double-crisis vertex is generated by the intersection of a grazing curve related to the sudden disappearance of chaotic orbits and a boundary crisis curve, which is called as a grazing-crisis vertex.

This paper demonstrates the existence of three types of crises in a single-degree-of-freedom piecewise linear oscillator. From the perspective of manifold tangency, the mechanisms of different crises are revealed, and critical exponents are determined to distinguish between homoclinic crises and heteroclinic crises. As the parameter continuously changes, chaotic orbits disappear abruptly at a certain critical point and reappear suddenly at another critical point. This phenomenon is related to the two tangencies of the stable and unstable manifolds of the boundary saddle. Besides we show that there are complex interactions between boundary crises and hysteresis, inducing transition repeatedly between a stable periodic orbit and a chaotic orbit.

The remaining structure is as follows. In Section 2, we give the mechanical model and the equations of motion. In Section 3, the theory of homoclinic crises and heteroclinic crises from the standpoint of manifold tangency proposed by Grebogi et al. is represented, and the concept of escape regions and intermittency regions formed by the intersection of manifolds after crises are introduced, and the mechanism of crisis disappearance is revealed using crisis-disappearance points in the two parameters domain. In Section 4, we reveal the dynamic behavior of the sudden disappearance and reappearance of chaotic orbits based on tangencies of the stable and unstable manifolds of the boundary saddle, and show and the presence of multiple boundary-crisis points can lead to a complex hysteresis phenomenon. Besides, crisis-disappearance points related to interior crises and merging crises are discovered, and the existence of crisis-disappearance points is demonstrated by numerical simulation. Section 5 gives a short summary.

2. Mechanical model

The single-degree-of-freedom piecewise linear oscillator is shown as in Fig. 1. There is a mass block M on the horizontal surface, and the displacement of the mass block M in the horizontal direction is denoted by X. When the displacement $X < 0$, the mass block M is connected to the wall through a linear spring K_1 and linear damping C. When the displacement is $X = 0$, the mass block M contacts with the linear spring K_2. The mass block M is subjected to an external force F.

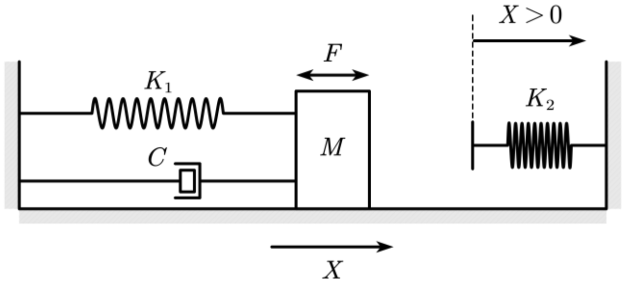

Fig. 1. A single-degree-of-freedom piecewise linear oscillator.

According to Newton's laws, the motion differential equation of the oscillator can be expressed as

$$M\ddot{X} + C\dot{X} + KX = F, \tag{1}$$

where K represents the stiffness, expressed as a piecewise linear function

$$K = \begin{cases} K_1, & X < 0, \\ K_1 + K_2, & X \geq 0. \end{cases} \tag{2}$$

When the external force $F = W + B\sin(\Omega t)$, this equation can be used to simulate the dynamics of a suspension bridge model[26], where W represents a constant force, B represents the amplitude of harmonic excitation, and Ω represents the frequency of harmonic excitation. Nondimensional parameters $x = XK_1 / W$, $\tau = t\sqrt{K_1 / M}$, $\omega = \Omega\sqrt{M / K_1}$, $2\xi = C / \sqrt{K_1 M}$, $k = K_2 / K_1$, $f = F / M$ are introduced. Let $x' = \mathrm{d}x / \mathrm{d}\tau$. The motion differential equation (1) can be rewritten as

$$\begin{cases} x' = y, \\ y' = f - 2\xi y - bx, \end{cases} \tag{3}$$

where

$$b = \begin{cases} 1, & x < 0, \\ 1 + k, & x \geq 0. \end{cases} \tag{4}$$

3. Crisis dynamics

In the following section 3.1 and 3.2, the theory of crises proposed by Grebogi et al.[9][10][27] will be discussed briefly, and we introduce the concept of the escape regions and the intermittency regions on this basis. In the section 3.3, we will give the concept of crisis-disappearance points.

3.1 Homoclinic crises and heteroclinic crises

Crises can be divided into homoclinic crises and heteroclinic crises based on the type of manifolds tangency. It should be noted that before the manifolds are tangent, the chaotic orbit lies on a branch of the unstable manifold but is not the closure of this branch. In other words, it is a subset of the closure of a certain unstable manifold branch associated with an unstable periodic orbit. It is only when tangency occurs that the chaotic orbit equals the closure of the unstable manifold branch.

3.2 Two types of regions related to crises

The concepts of boundary saddles (i.e., saddle orbits located on the basin boundary, denoted by BS) and interior saddles (i.e., saddle orbits located within the basin of attraction, denoted by IS) contribute to a deeper understanding of the crisis dynamics induced by the tangency of manifolds.

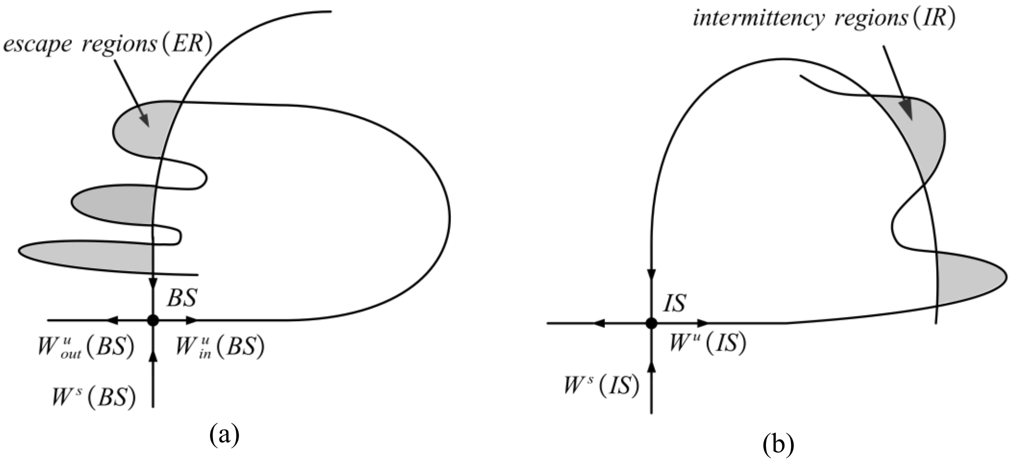

Fig. 2. The regions caused by the intersection of the stable and unstable manifolds of the unstable orbits after crises, (a) the escape regions; (b) the intermittency regions.

3.2.1 The escape regions.

As shown in Fig. 2(a), the stable and unstable manifolds of the boundary saddle BS are denoted by $W^s(BS)$ and $W^u(BS)$, respectively $W^u_{in}(BS)$ and $W^u_{out}(BS)$ represent unstable manifold branches located on the inner and outer sides of the basin of attraction of the chaotic orbit, respectively. After a boundary crisis, the unstable manifold intersects transversally with the stable manifold, creating the escape regions indicated by the shaded area. In fact, there are infinite such escape regions, because that once $W^s(BS)$ and $W^u(BS)$ intersect to one point, there will be infinite intersection points. If the initial point is chosen in the basin of the chaotic orbit before the crisis, the trajectory will be attracted by the chaotic orbit before the crisis for an arbitrary long time. This is almost indistinguishable from the chaotic orbit before the crisis, and this phenomenon is called chaotic transients[10]. The lifetime of chaotic transients is highly sensitive to initial condition. As time increases, the trajectory may leave the old region suddenly, enter an escape region ER along the direction of the stable manifold, and then leave the old region along the direction of $W^u_{out}(BS)$, ultimately being attracted by the attractor from other regions (infinity can also be considered as an attractor).

Let the critical parameter value for a boundary crisis occurrence be denoted as B^*, and the mean lifetime of chaotic transients be denoted as $\tau(\sigma)$. In a general case, assuming that the tangency between the stable manifold and the unstable manifold is quadratic, and the manifolds intersect with nonzero speed at the tangency. The variation of $\tau(\sigma)$ with respect to parameters can be expressed as[28]

$$A(\sigma) \sim b^{-\sigma}, \tag{5}$$

where

$$b = \left|B - B^*\right|. \tag{6}$$

σ is referred to as the critical exponent, depending on the type of manifold tangency during the crisis.

When the heteroclinic tangency occurs, we have

$$\sigma = \frac{1}{2} + (\ln\left|\alpha_1\right|)/\left|\ln\left|\alpha_2\right|\right|, \tag{7}$$

where α_1 and α_2 are the expanding $(|\alpha_1| > 1)$ and contracting $(|\alpha_2| < 1)$ eigenvalues, respectively.

When the homoclinic tangency occurs, we have

$$\sigma = (\ln\left|\beta_2\right|) / (\ln\left|\beta_1\beta_2\right|^2), \tag{8}$$

where β_1 and β_2 are the expanding $(|\beta_1| > 1)$ and contracting $(|\beta_2| < 1)$ eigenvalues, respectively.

3.2.2 The intermittency regions

Unlike boundary crises, interior crises are related to the interior saddle IS, but the basin boundary of the chaotic orbit is formed by the closure of the stable manifold of the boundary saddle BS. As shown in Fig. 2(b), the regions formed by the intersection of the stable manifold $W^s(IS)$ and the unstable manifold $W^u(IS)$ of the interior saddle IS after an interior crisis is referred to as the intermittency regions IR. Additionally, there is a return region, which is formed by the preimage of the chaotic orbit before the interior crisis. When the stable manifold of the interior saddle is tangent to its unstable manifold, the interior crisis occurs, and there is a sudden change in the size of the chaotic orbit.

For parameter values changes slightly after the crisis, the trajectory tends to stay on the chaotic orbit before the crisis. When the chaotic orbit accidentally enters an intermittency region IR, it moves towards the expanded region of the chaotic orbit along the direction of the stable manifold $W^s(IS)$. After a short stretch of bounce in the expanded region, the trajectory enters the return region and then returns to the original region, exhibiting an intermittency between expanded region and original region.

Merging crises is similar to interior cries, after the crisis point, the intersection of manifolds also creates intermittency regions, and the trajectory exhibits intermittently switches between the two-piece chaotic orbit before the crisis.

3.3 Crisis-disappearance points

In the case where the stable and unstable manifold of the same boundary saddle undergo two tangencies, it leads to the sudden disappearance and re-emergence of a chaotic orbit. With the changes of the parameter B, let D_B represent the distance between the two parameters where the tangency occur, so D_B can be defined as

$$D_B = \left| B_{BC_2} - B_{BC_1} \right|, \tag{9}$$

Where B_{BC_1}, B_{BC_2} represent the parameter values corresponding to the occurrences of the two boundary crises.

In the two-parameter space, varying parameters B and ξ simultaneously, the relationship between D_B and the parameters B and ξ can be illustrated by the schematic diagram in Fig. 3. In this diagram, the crisis curves C_{BC_1} and C_{BC_2} correspond to the boundary crises BC_1 and BC_2, respectively. Each point on curves C_{BC_1} and C_{BC_2} represents a tangency between the stable and unstable manifolds of a boundary saddle. The curves C_{BC_1} and C_{BC_2} coalesce and annihilate each other at a vertex. We call this vertex a crisis-disappearance point. Continuing to increase ξ beyond the crisis-disappearance point, the boundary crisis will no longer occur, so the chaotic orbit will persist. According to Ref. [23], we believe that there are infinitely many gaps caused by period windows on curves C_{BC_1} and C_{BC_2} .

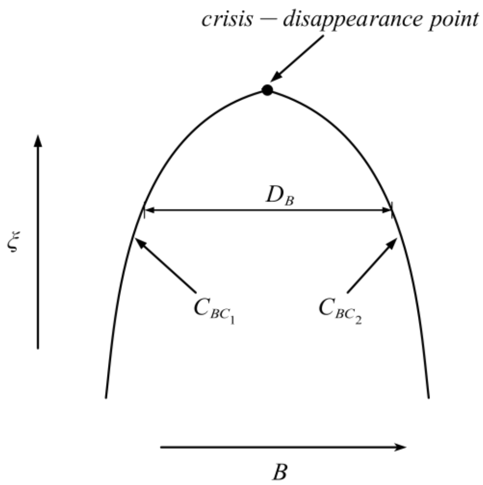

Fig. 3. A crisis-disappearance point.

4. Crisis dynamics of piecewise linear oscillators

In this Section, taking B as the bifurcation parameter and fixing some parameters of the system as $W = 1, \ k = 50, \ \omega = 0.6$, we investigate the crisis dynamics of the system for different values of ξ .

4.1. Boundary crises

4.1.1. ξ=0.073

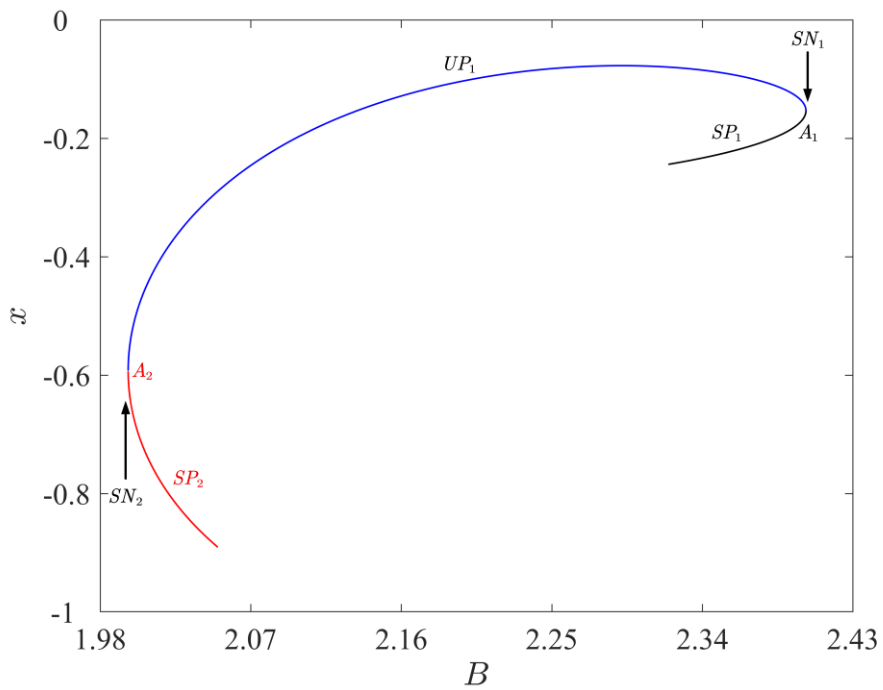

Fig. 4. Two saddle-node bifurcations generate the same unstable orbit UP , ξ =0.073.

As shown in Fig. 4, when ξ =0.073, saddle-node bifurcations SN_1 and SN_2 occur at $B = B_{SN_1}$ = 2.40187and $B = B_{SN_2}$ = 1.99671, respectively. These two saddle-node bifurcations generate the same unstable periodic orbit UP_1. Next, we will analyze the complex crisis dynamics of the two stable orbits A_1 and A_2.

Figure 5 shows the bifurcation diagram corresponding to the stable period-1 orbit SP_1 generated by saddle-node bifurcation SN_1 when the parameters B change continuously. As the parameter decreases to $B = B_{PD_1}$ = 2.17221, the stable period-1 orbit SP_1 undergoes the period-doubling bifurcation at PD_1, generating an unstable period-1 orbit UP_2 and a stable period-2 orbit. As the parameter continues to decrease, each branch of the stable period-2 orbit, through a period-doubling cascade, produces a chaotic band. The two chaotic bands collide with the unstable period-1 orbit UP_2 at MC_1 leading to a merging crisis, and the two chaotic bands merge into one. As the parameter decreases to $B = B_{IC_1}$ = 2.03834, the chaotic orbit resulting from the merging crisis collides with an unstable period-3 orbit UP_3 born in the saddle-node bifurcation SN_3, causing an internal crisis. The internal crisis makes the chaotic orbit to be in a larger-sized chaotic orbit CA_{11}. As the parameter continues to decrease to $B = B_{BC_1}$ = 2.0282696, the chaotic orbit collides with the unstable orbit UP_1, resulting in a boundary crisis BC_1. The chaotic orbit CA_{11} disappears abruptly. When the parameter decreases to $B = B_{BC_2}$ = 2.0128459, another boundary crisis BC_2 occurs, and the chaotic orbit CA_{12} reappears suddenly. The types and dynamical behaviors at each crises point are shown in Tab. 1.

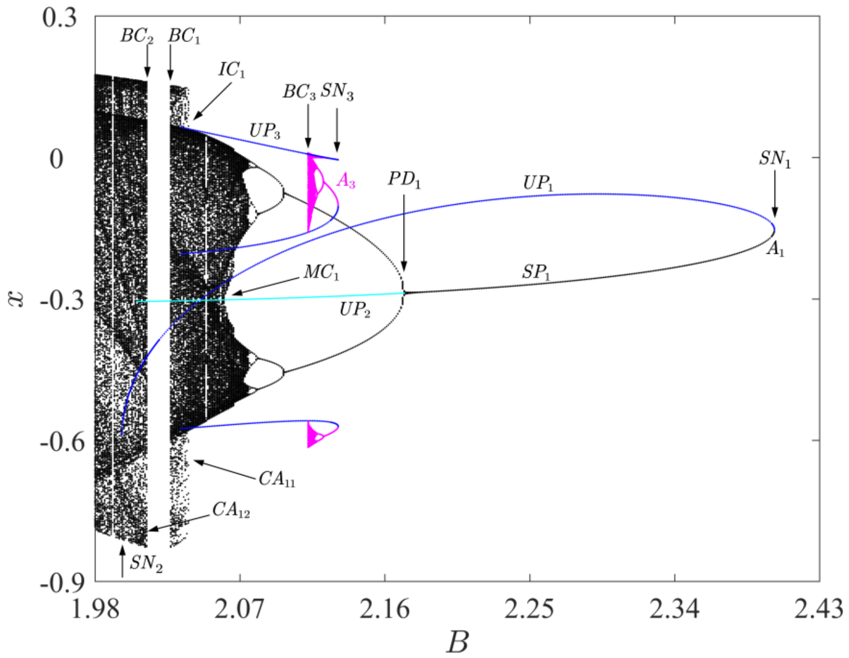

Fig. 5.The bifurcation diagram, $\xi = 0.073$ and $B \in [1.98.2.43]$.

Tab. 1. The corresponding crisis dynamics in Fig. 5.

Parameter value	Type of crises	Dynamics behavior
B_{BC_1}	Boundary crisis	Chaotic orbit CA_{11} collides with unstable orbit UP_1
B_{BC_2}	Boundary crisis	Chaotic orbit CA_{12} collides with unstable orbit UP_1
B_{BC_3}	Boundary crisis	Three-piece Chaotic orbit collides simultaneously with unstable orbit UP_3
B_{IC_1}	Interior crisis	Chaotic orbit collides with unstable orbit UP_3
B_{MC_1}	Merging crisis	Two-piece Chaotic orbit collides simultaneously with unstable orbit UP_2

Boundary crises BC_1 and BC_2 are both associated with unstable orbit UP_1. The stable manifold closure of UP_1 forms the basin boundary between stable orbits A_1 and A_2, so it belongs to the boundary saddle BS_1. Let the unstable manifold branch corresponding to the stable orbit A_1 be $W^s(BS_1)$, and the intersection of the stable manifold $W^s(BS_1)$ and the unstable manifold $W_1^u(BS_1)$ provides escape regions for chaotic transients after the crisis. As the parameter B increases, the area of escape regions also increases, leading to a greater possibility of escape for chaotic transients. Figure 8 shows how the mean lifetime τ of chaotic transients near two boundary crises depends on $|B - B_{BC}|$. Figure 6(a) (Fig. 6(b)) show the relationship between the mean lifetime of chaotic transients and the parameter value after the occurrence of boundary crisis BC_1 (before the occurrence of boundary crisis BC_2). In the log-log scale plot, the critical exponent corresponds to the slope of the line, and the blue dashed line represents the fitted result. Table 2 presents critical exponents fitted and calculated by Eqs. (7) and (8). σ_1 and σ_2 represent the critical exponents corresponding to boundary crises BC_1 and BC_2 , respectively. By comparing the results of numerical fitting with the theoretical calculation, it is shown that BC_1 belongs to the heteroclinic crisis, while BC_2 belongs to the homoclinic crisis.

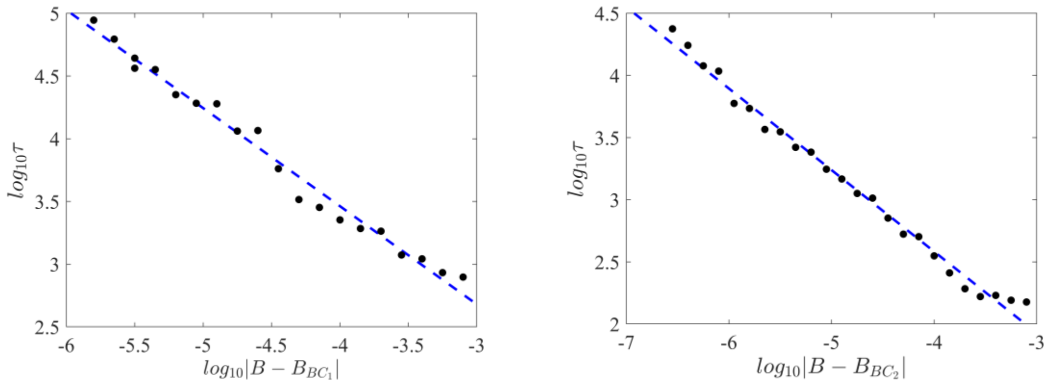

(a) (b)

Fig. 6. The mean lifetime of chaotic transients, (a) after the occurrence of boundary crisis BC_1; (b) before the occurrence of boundary crisis BC_2.

Tab. 2. The critical exponents corresponding to BC_1, BC_2.

Critical exponents	Numerical fitting	Heteroclinic crisis	Homoclinic crisis
σ_1	0.7821	0.7590	0.6747
σ_2	0.6558	0.7223	0.6429

Figures 7 and 8 present the manifold diagrams at boundary crises BC_1 and BC_2 , respectively. As shown in Fig. 7, the stable manifold $W^s(BS_1)$ of the boundary saddle BS_1 (i.e., unstable orbit UP_1) undergoes a heteroclinic tangency with the unstable manifold $W^u(IS_1)$ of the internal saddle IS_1 (i.e., unstable orbit UP_2) born in the period-doubling bifurcation PD_1 . This leads to a sudden disappearance of the chaotic orbit CA_{11}. Here, the chaotic orbit CA_{11} is not only the closure of the unstable manifold branch $W^u(IS_1)$, but also the closure of the unstable manifold branch $W_1^u(BS_1)$. As shown in Fig. 8, the homoclinic tangency of the stable manifold $W^s(BS_1)$ and the unstable manifold branch $W_1^u(BS_1)$ causes the reappearance of disappeared chaotic orbit CA_{11}, forming a chaotic orbit

CA_{12}. The phenomenon of the chaotic orbit CA_{11} suddenly disappearing and then reappearing can be explained from the perspective of manifolds. For $B > B_{BC_1}$, the unstable manifold branch $W_1^u(BS_1)$ of the chaotic orbit CA_{11} is within basin boundary formed by the closure of the stable manifold $W^s(BS_1)$ .After the merging crisis MC_1 occurs, the chaotic orbit always is the closure of the unstable manifold $W^u(IS_1)$. The tangency of the stable manifold $W^s(BS_1)$ with the unstable manifold branch $W^u(IS_1)$ ($W_1^u(BS_1)$) causes a heteroclinic crisis at $B = B_{BC_1}$. As B further decreases, the stable manifold $W^s(BS_1)$ intersects with the unstable manifold $W_1^u(BS_1)$, forming escape regions. The area of the escape regions exhibits a pattern of increasing and then decreasing as the parameter B decreases. When B decreases to $B = B_{BC_2}$, the area of escape regions decreases to zero, and the stable manifold $W^s(BS_1)$ and the unstable manifold $W_1^u(BS_1)$ are homoclinically tangent. Once the homoclinic crisis occurs, the chaotic orbit CA_{12} reappears.

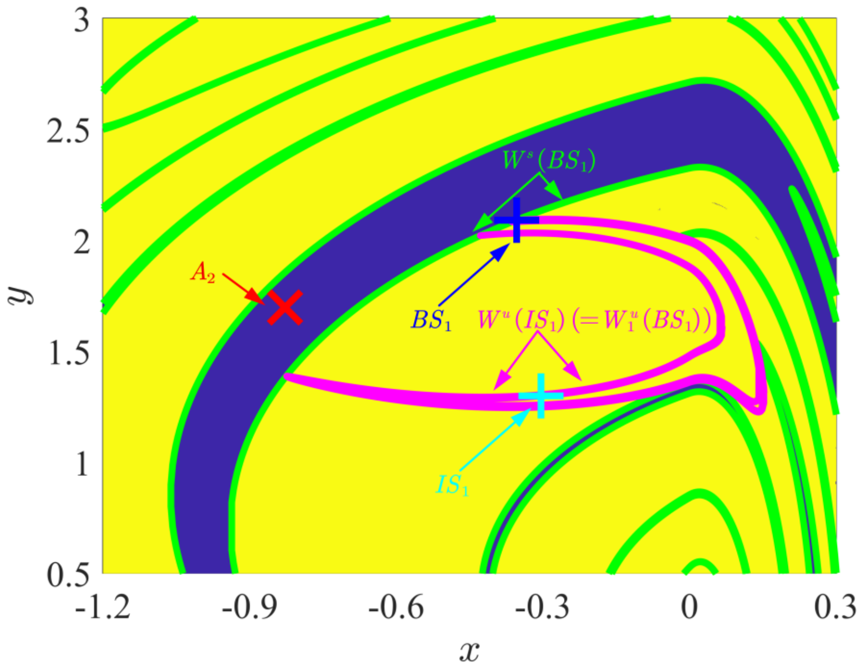

Fig. 7. The heteroclinic tangency between the unstable manifold $W^u(IS_1)$ of the interior saddle IS_1 and the stable manifold $W^s(BS_1)$ of the boundary saddle BS_1, $B = B_{BC_1}$.

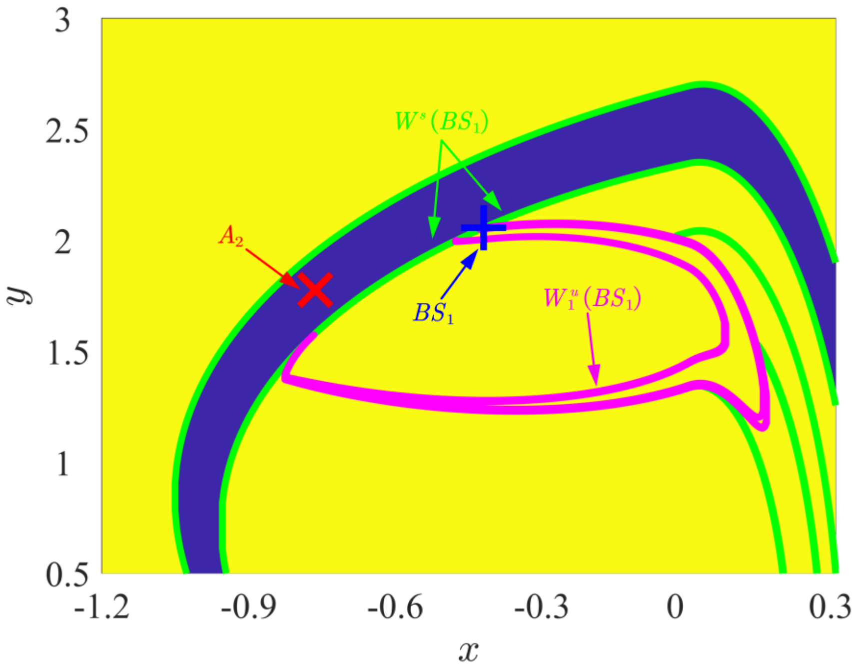

Fig. 8. The homoclinic tangency between the stable manifold $W^s(BS_1)$ and the unstable manifold branch $W_1^u(BS_1)$ of the boundary saddle BS_1, $B = B_{BC_2}$.

The coexistence of stable orbits A_2, A_4 is illustrated in Fig. 9. Similarly, for stable orbits A_2, as the parameter B increases, firstly, a stable period-1 orbit SP_2 undergoes a period-doubling cascade into a chaotic orbit CA_{21}. This chaotic orbit collides with an unstable orbit UP_1 at $B_{BC_4} = 2.2057122$, leading to a boundary crisis BC_4, and the chaotic orbit CA_{21} abruptly disappears. When B increases to $B_{BC_5} = 2.3926124$, boundary crisis BC_5 occurs, and the chaotic orbit CA_{22} reappears.

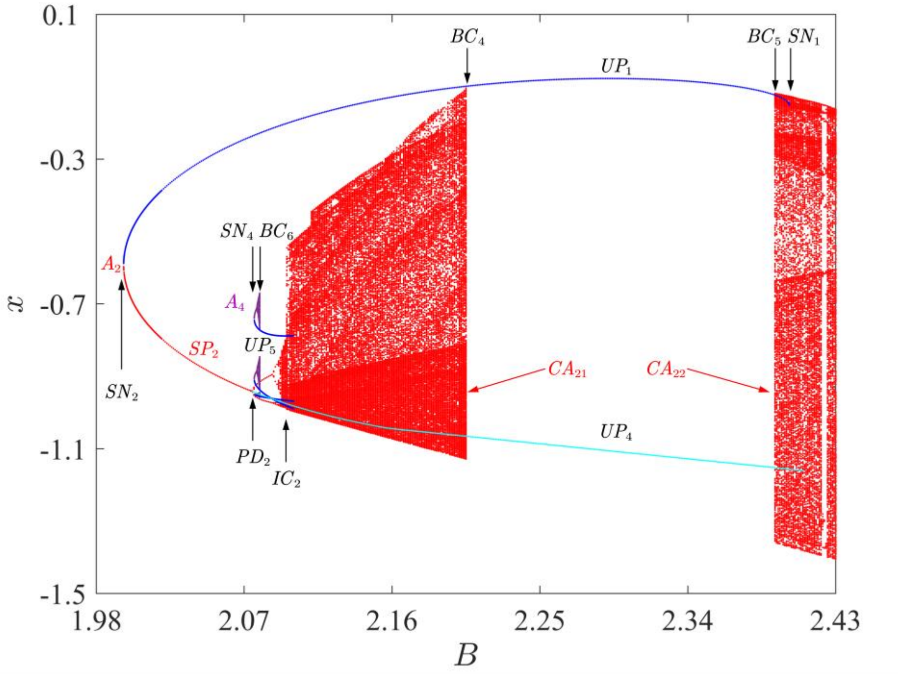

Fig. 9. The bifurcation diagram, $\xi = 0.073$ and $B \in [1.98.2.43]$.

Tab. 3. The corresponding crisis dynamics in Fig. 9.

Parameter value	Type	Dynamics behavior
B_{BC_4}	Boundary crisis	Chaotic orbit CA_{21} collides with unstable orbit UP_1
B_{BC_5}	Boundary crisis	Chaotic orbit CA_{22} collides with unstable orbit UP_1
B_{BC_6}	Boundary crisis	Three-piece Chaotic orbit collides simultaneously with unstable orbit UP_5
B_{IC_2}	Interior crisis	Chaotic orbit collides with unstable orbit UP_5

In the log-log scale plot, Fig. 10(a) (Fig. 10(b)) shows the relationship between the mean lifetime of chaotic transients and the parameter value after the occurrence of the boundary crisis BC_4 (before the occurrence of the boundary crisis BC_5). Table 2 presents critical exponents fitted and calculated by Eqs. (7) and (8). σ_4 and σ_5 represent the critical exponents corresponding to boundary crises BC_4 and BC_5, respectively. By comparing the results of numerical fitting with the theoretical calculation, it is shown that BC_4 belongs to the heteroclinic crisis, while BC_5 belongs to the homoclinic crisis.

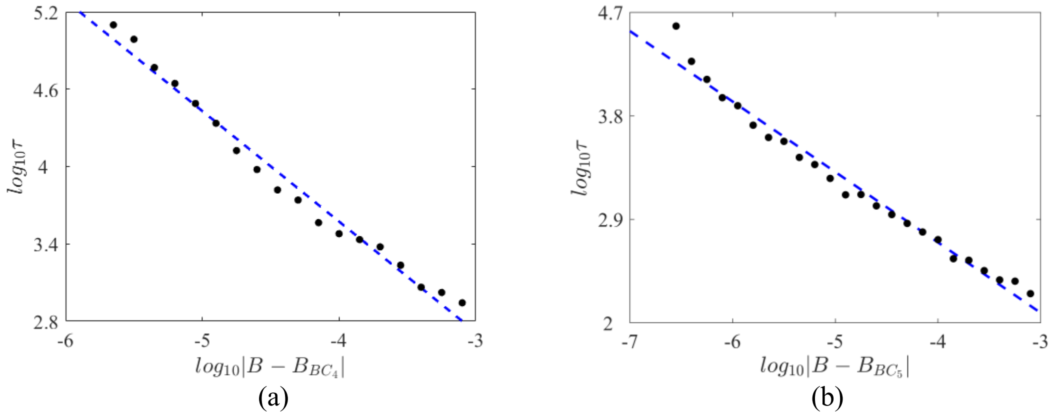

Fig. 10. The mean lifetime of chaotic transients, (a) after the occurrence of boundary crisis BC_4; (b) before the occurrence of boundary crisis BC_5.

Tab. 4. The critical exponents corresponding to BC_4, BC_5.

Critical exponent	Numerical fitting	Heteroclinic crisis	Homoclinic crisis
σ_4	0.8574	0.8344	0.7512
σ_5	0.6123	0.6872	0.6152

Figures 11 and 12 give the manifold diagrams corresponding to BC_4 and BC_5, respectively. As shown in Fig. 11, the stable manifold $W^s(BS_1)$ of the boundary saddle BS_1 (i.e., unstable orbit UP_1) and the unstable manifold $W^u(IS_2)$ of the internal saddle IS_2 (i.e., unstable orbit UP_4) born in the period-doubling bifurcation PD_2 undergoes a heteroclinic tangency, causing the sudden disappearance of the chaotic orbit CA_{21}. Simultaneously, the chaotic orbit CA_{21} is the closure of the unstable manifold $W^u(IS_2)$ and the closure of the unstable manifold branch $W_2^u(BS_1)$. As shown in Fig. 12, the unstable manifold branch $W_2^u(BS_1)$ of the boundary saddle BS_1 and its stable manifold $W^s(BS_1)$ have a homoclinic tangency, leading to the reappearance of the disappeared chaotic orbit CA_{21}, forming a chaotic orbit CA_{22}.The process of the chaotic orbit CA_{21} suddenly disappearing and then reappearing is also caused by the change in the area of escape regions formed by the intersections of manifolds.

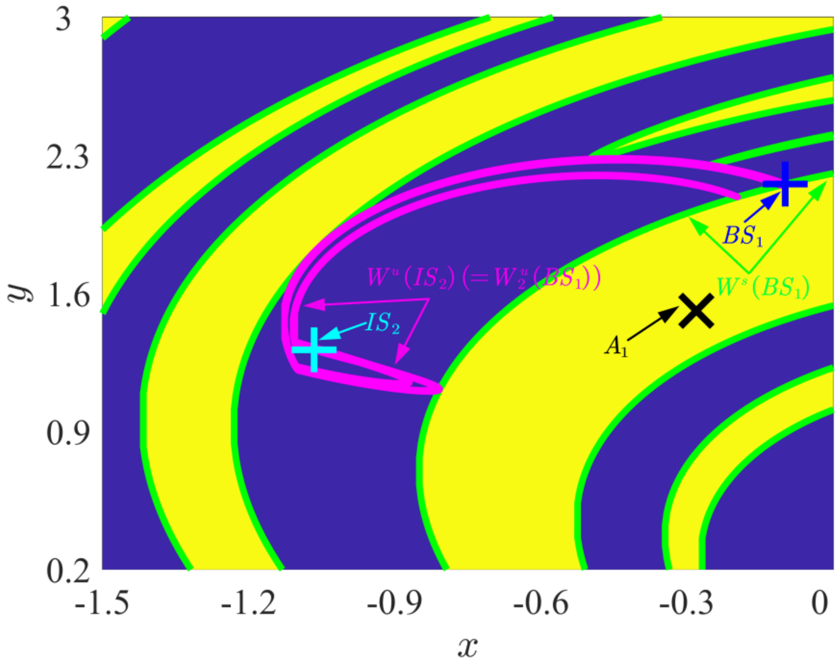

Fig. 11. The heteroclinic tangency between the unstable manifold $W^u(IS_2)$ of the interior saddle IS_2 and the stable manifold $W^s(BS_1)$ of the boundary saddle BS_1, $B = B_{BC_4}$.

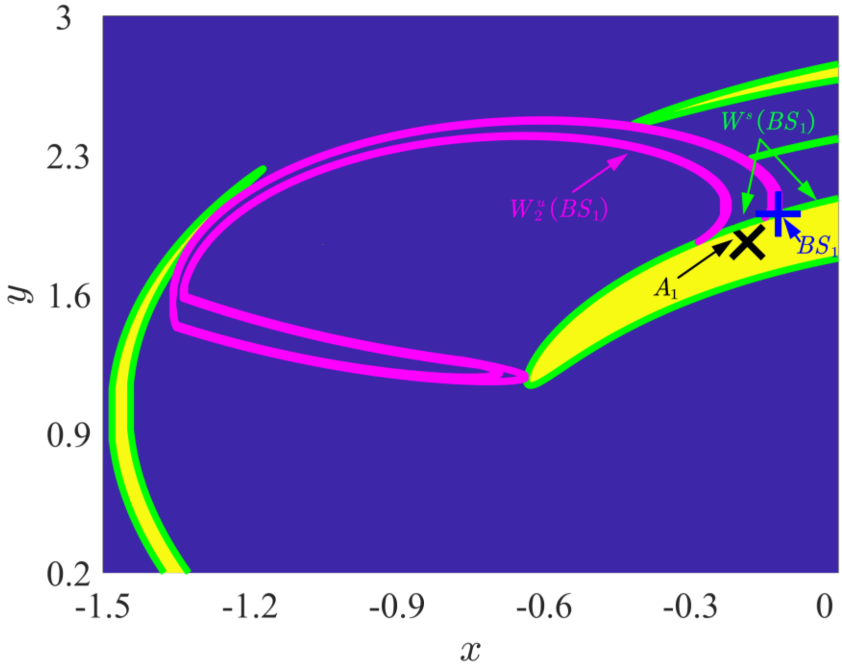

Fig. 12. The homoclinic tangency between the stable manifold $W^s(BS_1)$ and the unstable manifold $W_2^u(BS_1)$ of the boundary saddle BS_1, $B = B_{BC_5}$.

As chaotic orbits suddenly disappearing and reappearing in the orbits A_1 and A_2, the stable manifold $W^s(BS_1)$ of the boundary saddle BS_1 and its two unstable manifold branches $W_1^u(BS_1)$, $W_2^u(BS_1)$ both undergo two tangencies as the parameter B continuously changes.

The bifurcation diagram in Fig. 13 is the combination of Fig. 5 and Fig. 9. It is shown that two stable orbits A_1 and A_2 exhibit a complex hysteresis effect in the region $B \in [B_{SN_2}, B_{SN_1}]$. Due to boundary crises caused by collisions with UP_1, the corresponding chaotic orbits of the two stable orbits A_1 and A_2 are interrupted in intervals $B \in [B_{BC_2}, B_{BC_1}]$ and $B \in [B_{BC_4}, B_{BC_5}]$, respectively. Consequently, the dynamics of system exhibit complex hysteresis behaviors.

(1) Along the direction of the increasing parameter B: As B =1.98, the steady state is the chaotic orbit CA_{12} (on A_1); as the parameter increases to the boundary bifurcation BC_2, CA_{12} suddenly disappears, and the stable state transitions from CA_{12} to the period-1 orbit SP_2 (on A_2), Subsequently, SP_2 goes through a period-doubling cascade, leading to the formation of the chaotic orbit CA_{21} (on A_2) ;When the parameter increases to another boundary crisis BC_4, CA_{21} is disrupted, and the stable state transitions from CA_{21} to another period-1 orbit SP_1 (on A_1); As the parameter continues to increase, and surpasses the saddle-node bifurcation SN_1, the system transitions back to the chaotic orbit CA_{22} (on A_2). The transition relationship of the steady state is as follows:

Chaotic orbit CA_{12} (on A_1) $\xrightarrow{BC_2}$ Period-1 orbit SP_2 (on A_2) $\xrightarrow{period-doubling\ cascade}$ Chaotic orbit CA_{21} (on A_2) $\xrightarrow{BC_4}$ Period-1 orbit SP_1 (on A_1) $\xrightarrow{SN_1}$ Chaotic orbit CA_{22} (on A_2)

(2) Similarly, along the direction of decreasing parameter B, the transition relationship of the steady state is as follows:

Chaotic orbit CA_{22} (on A_2) $\xrightarrow{BC_5}$ Period-1 orbit SP_1 (on A_1) $\xrightarrow{period-doubling\ cascade}$ Chaotic orbit CA_{11} (on A_1) $\xrightarrow{BC_1}$ Period-1 orbit SP_2 (on A_2) $\xrightarrow{SN_2}$ Chaotic orbit CA_{12} (on A_1)

In summary, within the hysteresis region $B \in [B_{SN_2}, B_{SN_1}]$, due to boundary crises, the chaotic orbits associated with the coexisting stable orbits A_1 and A_2 are disrupted, leading to a dynamic transition phenomenon inside the hysteresis region. This means that there is a mutual transition of dynamic states among the orbits A_1 and A_2.

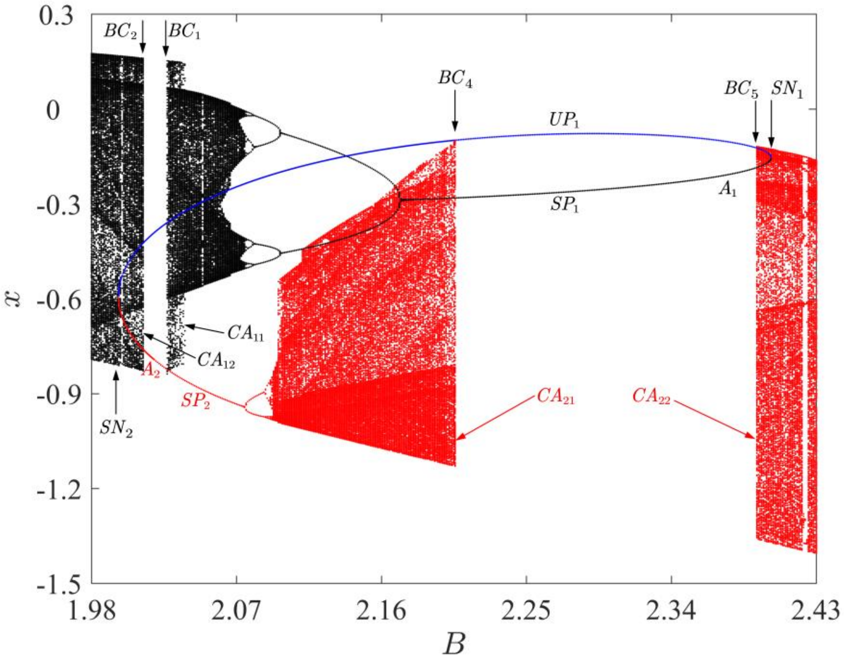

Fig. 13. The complex impact of crisis dynamics on hysteresis effects, $B \in [1.98, 2.43]$.

4.1.2. *ξ*=0.075

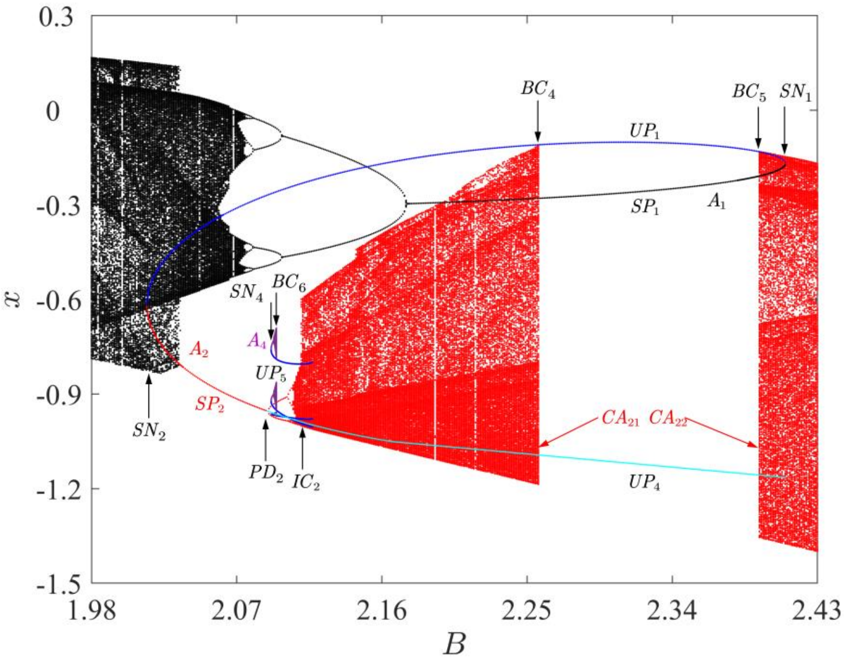

Fig. 14. The bifurcation diagram when $\xi = 0.075$ and $B \in [1.98.2.43]$.

When ξ increases to 0.075, the bifurcation diagram is shown in Fig. 14. Boundary crises BC_1, BC_2 disappears, indicating that it exceeds the crisis-disappearance point associated with the boundary crisis BC_1, BC_2. For the stable orbit A_1, the stable manifold $W^s(BS_1)$ of the boundary saddle BS_1 no longer has a tangency with its unstable manifold branch $W_1^u(BS_1)$, and the stable orbit A_1 persists in the given parameter range. The phenomenon of the sudden disappearance and reappearance of chaotic orbits indicates that the existence of crisis-disappearance point is related to boundary crises.

4.1.3. ξ =0.0773

In the previous bifurcation diagrams, with the increase of parameter ξ, the boundary crises BC_1, BC_2 related to stable orbit A_1 disappear, and the distance between the boundary crises BC_4, BC_5 related to stable orbit A_2 decreases. The parameter values at which boundary crises BC_4, BC_5 disappear can be determined.

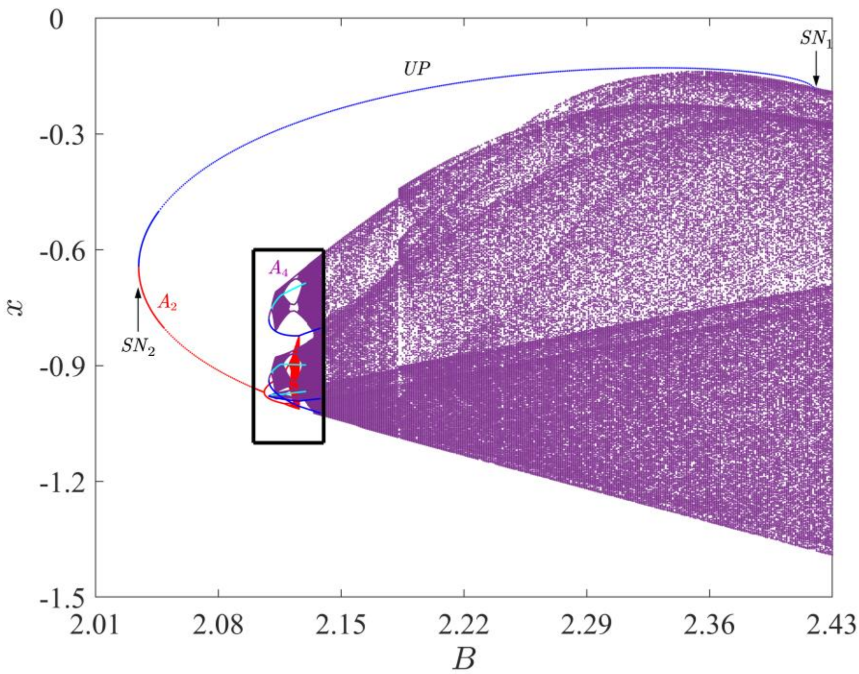

(a)

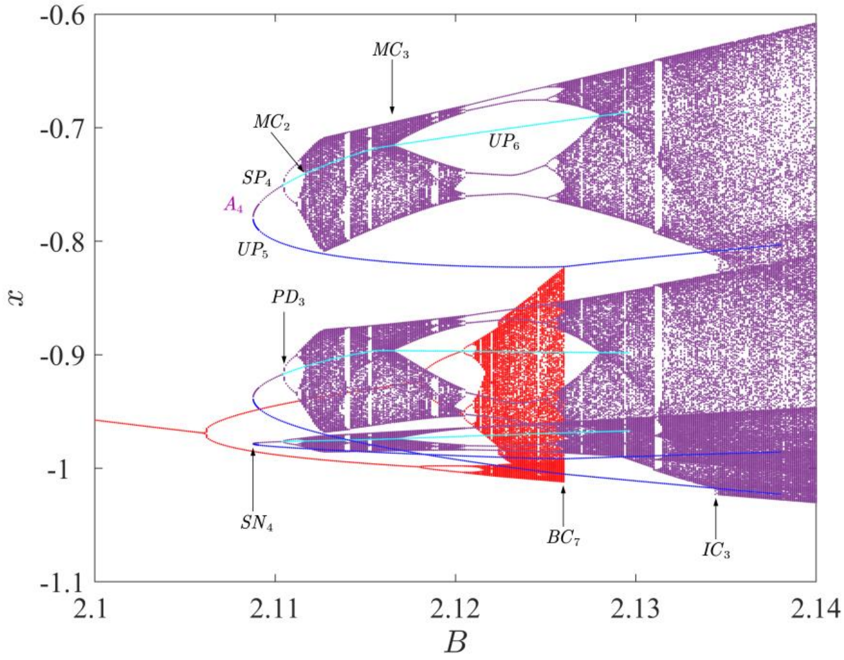

(b)

Fig. 15 The bifurcation diagram at $\xi = 0.0773$, (a) $B \in [2.01, 2.43]$; (b) $B \in [2.1, 2.14]$.

Tab. 5. The corresponding crisis dynamics in Fig. 15.

Parameter value	Type	Dynamics behavior
B_{BC_7}	Boundary crisis	Chaotic orbit collides with unstable orbit UP_5
B_{IC_3}	Interior crisis	Three-piece Chaotic orbit collides simultaneously with unstable orbit UP_5
B_{MC_2}	Merging crisis	Two-piece Chaotic orbit collides simultaneously with unstable orbit UP_6
B_{MC_3}	Merging crisis	Two-piece Chaotic orbit collides simultaneously with unstable orbit UP_6

The bifurcation diagram at ξ = 0.0773 is shown in Fig. 15. The partial enlargement corresponding to the marked region in Fig. 17(a) is depicted in Fig. 17(b). The saddle-node bifurcation SN_4 at B =2.10878 induces a stable period-3 orbit SP_4 . This orbit SP_4 occupies a region within the basin of attraction of the stable orbit A_2 . The stable manifold closure of the unstable period-3 orbit UP_5 forms the basin boundary of the stable orbit A_4 , so UP_5 is referred as the boundary saddle BS_2 . As the parameter B increases continuously, SP_4 evolves into a three-piece chaotic orbit through a period-doubling cascade. Before $B = B_{BC_6}$ =2.12604, the unstable orbit UP_5 did not collide with the stable orbit A_4, because that it has already exceeded the crisis-disappearance point associated with the unstable orbit UP_5. Since the stable orbit A_4 is not disrupted as the parameter B continues to increase, the basin of attraction for the stable orbit A_4 also increases. As shown in Fig. 16, the chaotic orbit corresponding to the stable orbit A_2 collides with BS_2 and collides with the basin boundary of A_4 at $B = B_{BC_7}$ simultaneously. As the boundary crisis BC_7 occurs, and the stable orbit A_2 and its basin of attraction suddenly disappears. The basin of attraction of A_2 is rapidly occupied by the basin of attraction of A_4, so the boundary saddle BS_2 corresponding to the unstable period-3 orbit born in SN_4 transforms into an interior saddle IS_3. As shown in Fig. 17, when $B = B_{IC_3}$ =2.13427, the chaotic orbit formed by A_4 collides with the interior saddle IS_3. Interior crisis IC_3 occurs, and the chaotic orbit suddenly expands. During the parameter B increase to SN_1 continuously, the chaotic orbit does not collide with the unstable orbit UP_1, so the boundary crises BC_4 and BC_5 disappears.

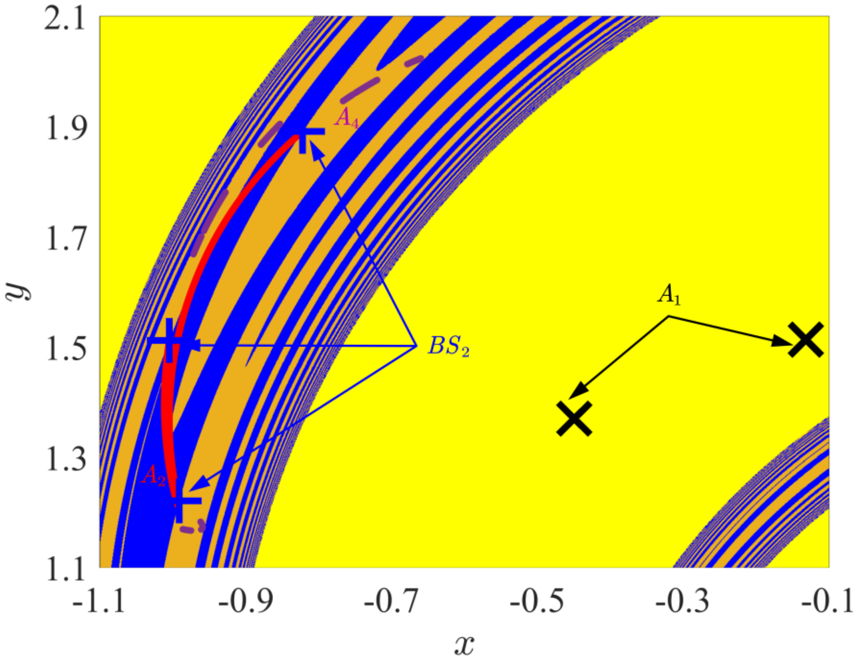

Fig. 16. Stable orbit A_2 collides with boundary saddle BS_2 at boundary crisis BC_7, $B = B_{BC_7}$.

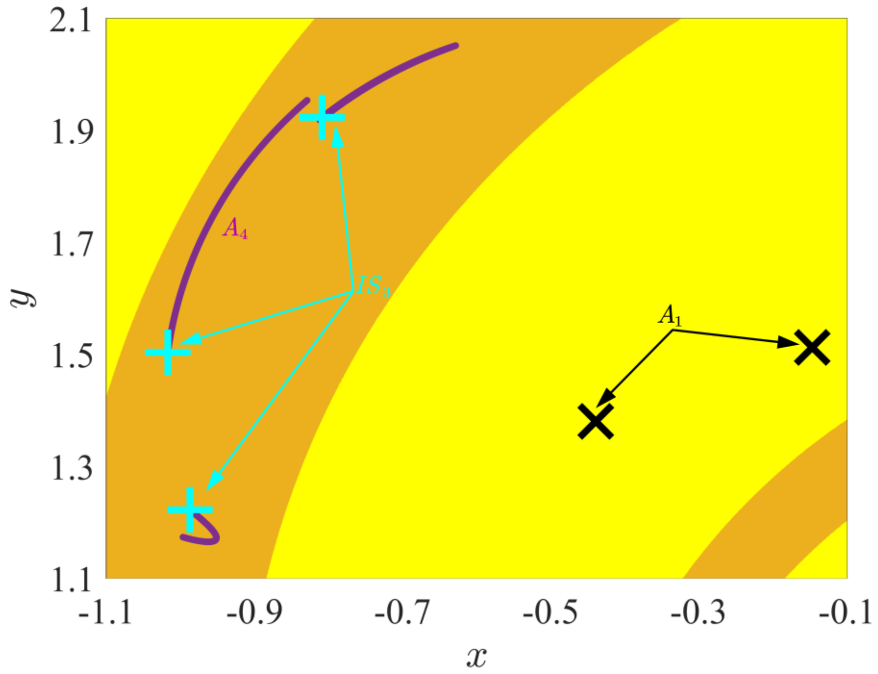

Fig. 17. Stable orbit A_4 collides with interior saddle IS_3 at interior crisis IC_3, $B = B_{IC_3}$.

4.2 Interior crises and merging crises

As shown in Fig. 15(b), there is a merging crisis MC_3 , leading to the sudden splitting of chaotic orbits that merged at a merging crisis MC_2 . This process is similar to the phenomenon described earlier, where a chaotic orbit suddenly disappears and then reappears. Merging crises MC_2 and MC_3 are both related to the unstable periodic orbit UP_6 born in the period-doubling bifurcation PD_3 . Similarly, we can examine this process by the changes in the area of intermittency regions formed by the intersection of the stable and unstable manifolds of the unstable periodic orbit UP_6 . The stable and unstable manifolds of the unstable periodic orbit UP_6 undergo the first tangency at $B = B_{MC_2}$, resulting in the sudden merging of a chaotic orbit. Beyond a critical value B_{MC_2} , the intersections of the manifolds forms intermittency regions. As the parameter continues to increase, the area of these regions grows initially and then decreases. When $B = B_{MC_3}$, the area of the intermittency regions becomes zero, indicating the second tangency of the manifolds. This causes the sudden splitting of the previously merged chaotic orbit.

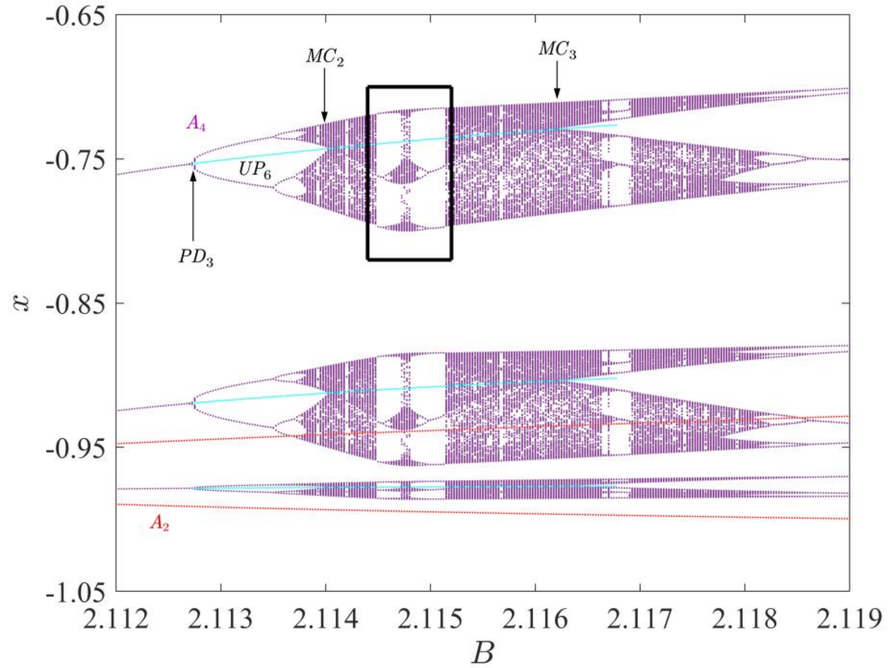

(a)

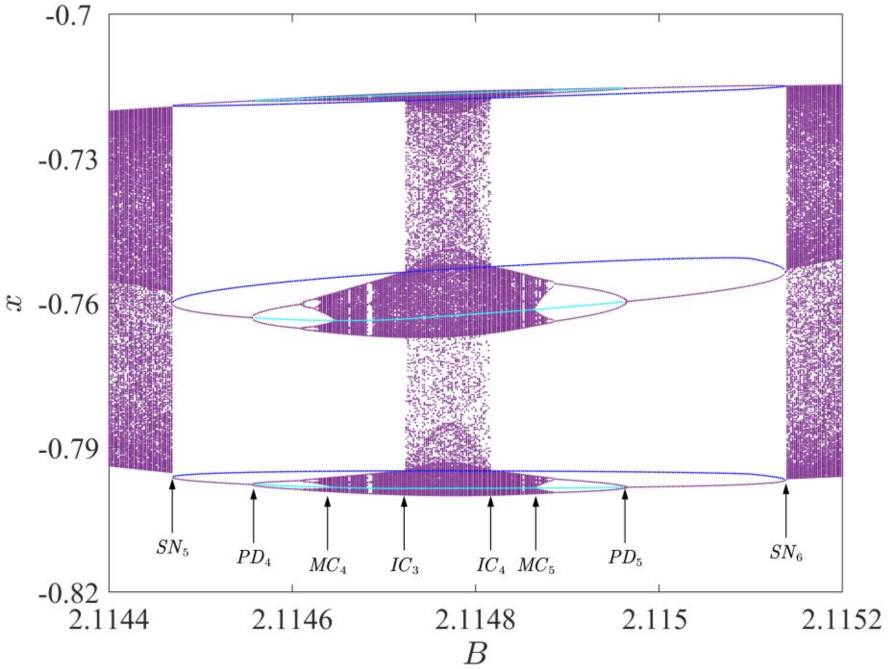

(b)

Fig. 18. The bifurcation diagram at $\xi = 0.0776$, (a) $B \in [2.111, 2.119]$; (b) $B \in [2.1144, 2.1152]$.

Tab. 6. The corresponding crisis dynamics in Fig. 18.

Parameter value	Type	Dynamics behavior
B_{IC_4}	Interior crisis	Nine-piece Chaotic orbit collides simultaneously with unstable orbit UP_8
B_{IC_5}	Interior crisis	Nine-piece Chaotic orbit collides simultaneously with unstable orbit UP_8
B_{MC_4}	Merging crisis	Eighteen-piece Chaotic orbit collides simultaneously with unstable orbit UP_7
B_{MC_5}	Merging crisis	Eighteen-piece Chaotic orbit collides simultaneously with unstable orbit UP_7

When parameter ξ =0.0776, the corresponding bifurcation diagram is shown in Fig. 18. Figure 18(b) provides a partial enlargement of Fig. 18(a). This represents a "special" period window: the unstable orbit UP_8 between the period-doubling bifurcations PD_4 and PD_5 leads to the sudden merging of chaotic orbit at the merging crisis MC_4 , and re-split at the merging crisis MC_5 . In this window, a similar process is observed for interior crises. The collision between the unstable orbit UP_7 and a chaotic orbit between the saddle-node bifurcations SN_5 and SN_6 leads to the occurrence of interior crises IC_4 and IC_5 . The interior crisis IC_4 causes a sudden expansion in the size of the chaotic orbit. As the parameter B increases, an interior crisis IC_5 results in the previously enlarged chaotic crisis to shrink suddenly. This process of the sudden expansion and shrinking in a chaotic orbit is explained by examining the change in the area of intermittency regions formed when the stable manifold of the interior saddle intersects with its unstable manifold.

The occurrence of merging crises MC_2, MC_3, MC_4, MC_5 and interior crises IC_4, IC_5 indicates the existence of crisis-disappearance points related to merging crises and interior crises. There are infinite such "special" periodic windows, but as the period increases, their existence intervals become smaller and harder to observe. This also suggests that there is more than one crisis-disappearance point associated with merging crises and interior crises.

4.3 Crisis- disappearance points in parameter space (*ξ*,*B*)

The case of two parameters is considered. Let $D_{B_1} = |B_{BC_4} - B_{BC_5}|$ corresponding to different damping coefficient ξ , as shown in Tab. 7. With the increase of ξ , although the parameter values for boundary crises may change, their distance shows a decreasing trend. The mean lifetime of chaotic transients is related to the area of escape regions. When D_{B_1} reaches a very small value, the relationship between the area of escape regions and the parameter B does not satisfy Eq. (5). It is worth noting that when $\xi = 0.0767$, boundary crisis BC_6 have already occurred. When ξ changes from 0.0765 to 0.077, the amplitude of the change in D_{B_1} becomes larger, which may be related to crisis dynamics caused by the appearance of boundary crisis BC_6 .

Tab. 7. The parameter distance D_{B_1} corresponding to different damping coefficient ξ .

ξ	B_{BC_4}	B_{BC_5}	$D_{B_1} = \left\| B_{BC_5} - B_{BC_4} \right\|$
0.075	2.256	2.395	0.139
0.0755	2.270	2.393	0.123
0.076	2.281	2.390	0.109
0.0765	2.308	2.383	0.075
0.077	2.339	2.366	0.027
0.07707	2.351	2.355	0.004

Simultaneously, by the variation of the maximum area $A_{\max}(B)$ of escape regions, the existence of the crisis-disappearance point can be determined. As ξ increases, $A_{\max}(B)$ also exhibits a decreasing trend. Although it is not possible to determine at which point the area of escape regions reaches its maximum value, the trends of equivalent in $A_{\max}(B)$ can be determined by the changes in the area of the escape region produced by the intersection of the stable and unstable manifolds of the boundary saddle at the midpoint of the interval $[B_{BC_1}, B_{BC_2}]$ at different ξ , as shown in Fig. 19. It is evident that with a decrease in ξ , the area of escape regions also decreases. The likelihood of trajectories escaping from the region where chaotic orbits existed originally decrease, leading to a reduction in the lifetime of chaotic transients.

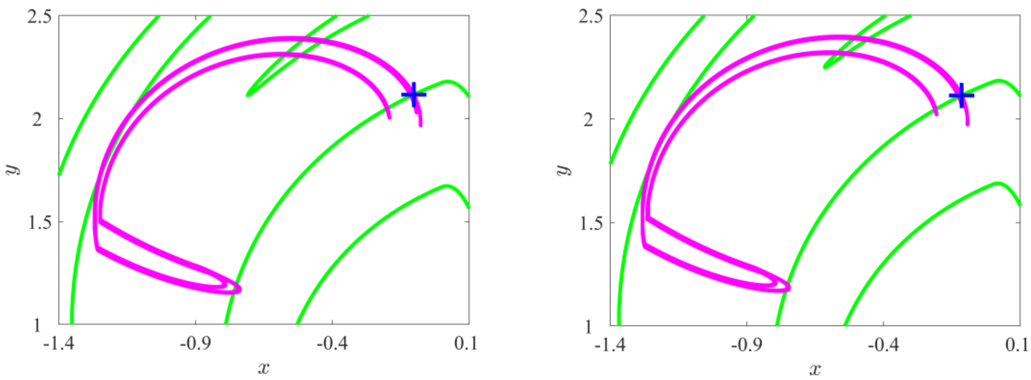

(a) (b)

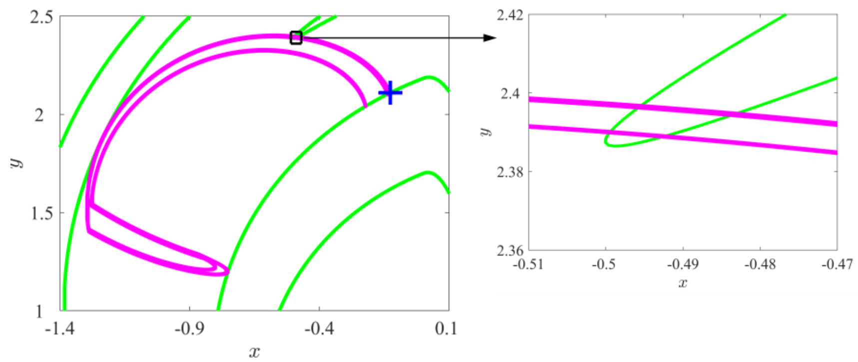

(c)

Fig. 19. The change of escape regions under different parameter (ξ, B) , (a) $\xi = 0.075$, $B = 2.3255$; (b) $\xi = 0.076$, $B = 2.3355$; (c) $\xi = 0.077$, $B = 2.3525$.

$D_{B_2} = \left| B_{MC_2} - B_{MC_3} \right|$ is used to represent the parameter distance of merging crises MC_2, MC_3 . It is shown that D_{B_2} exhibits a decreasing trend with an increase in ξ . Table 8 gives the numerical results for D_{B_2} corresponding to different parameter.

Tab. 8. The change of D_{B_2} with the variation of ξ .

ξ	B_{MC_2}	B_{MC_3}	D_{B_2}
0.0772	2.1108	2.1170	0.0062
0.0775	2.1135	2.1164	0.0029
0.0779	2.1165	2.1171	0.0006

5. Conclusions

We focus on the crisis dynamics in a class of single-degree-of-freedom piecewise-linear oscillators. From the perspective of manifolds, it is shown that the sudden disappearance and reappearance of a chaotic orbit are related to boundary crises caused by collisions between the chaotic orbit and the same unstable periodic orbit, and the types of these two boundary crises are different. By comparing the numerical relationship between the mean lifetime of chaotic transients and parameter values with the result of theoretical calculations, it is shown that one of these two boundary crises belongs to a homoclinic crisis, while the other belongs to heteroclinic crisis. Furthermore, by changing two parameters simultaneously, two boundary-crisis curves related to the same unstable periodic orbit will produce a coalescence point that we name the crisis-disappearance point. We also identify crisis-disappearance points related to interior crises and merging crises.

Due to the presence of boundary crises, the hysteresis phenomenon will exhibit a more complex form, inducing transition repeatedly between two stable orbits. There are complex dynamical transition not only on the hysteresis boundary, but also within the hysteresis region, the chaotic orbits coexisting with periodic orbits may be destroyed or generated. This leads to the occurrence of complex dynamical transitions within the hysteresis region. Generally, in engineering, dynamical systems should avoid dynamical transitions as much as possible. However, these transitions are widespread in dynamical systems. The results of this detailed study can provide a guidance for the optimization design of dynamical systems.

Ackonwledgments

This work is supported by the National Natural Science Foundation of China (NSFC) (Nos. 12072291 and 12172306).

References

[1] Alzubaidi B, Németh R K. Modal analysis-based calculation of periodic nonlinear responses of harmonically forced piecewise linear elastic systems. Journal of Sound and Vibration, 2023, 549: 117576.

[2] Gonçalves J M. Regions of stability for limit cycle oscillations in piecewise linear systems. IEEE Transactions on Automatic Control, 2005, 50(11): 1877-1882.

[3] Liu R, Grebogi C, Yue Y. Double grazing bifurcation route in a quasiperiodically driven piecewise linear oscillator. Chaos: An Interdisciplinary Journal of Nonlinear Science, 2023, 33(6):063150.

[4] Kong C, Liu X B. Noise-induced chaos in a piecewise linear system. International Journal of Bifurcation and Chaos, 2017, 27(9): 1750137.

[5] Afzali F, Kharazmi E, Feeny B F. Resonances of a forced van der Pol equation with parametric damping. Nonlinear Dynamics, 2023, 111(6): 5269-5285.

[6] Jayaprakash K R, Tandel V, Starosvetsky Y. Dynamics of excited piecewise linear oscillators. Nonlinear Dynamics, 2023, 111(6): 5513-5532.

[7] Pei L, Chong A S E, Pavlovskaia E, Wiercigroch M. Computation of periodic orbits for piecewise linear oscillator by harmonic balance methods. Communications in Nonlinear Science and Numerical Simulation, 2022, 108: 106220.

[8] Wang Q, Yan Z, Dai H. An efficient multiple harmonic balance method for computing quasi-periodic responses of nonlinear systems. Journal of Sound and Vibration, 2023, 554: 117700.

[9] Grebogi C, Ott E, Yorke J A. Chaotic attractors in crisis. Physical Review Letters, 1982, 48(22): 1507-1510.

[10] Grebogi C, Ott E, Yorke J A. Crises, sudden changes in chaotic attractors, and transient chaos. Physica D: Nonlinear Phenomena, 1983, 7(1-3): 181-200.

[11] Yang H L, Huang Z Q, Ding E J. Early crisis induced in maps with parametric noise. Physical review letters, 1996, 77(24): 4899-4902.

[12] Finardi M, Flepp L, Parisi J, Holzner R, Badii R, Brun E. Topological and metric analysis of heteroclinic crisis in laser chaos. Physical review letters, 1992, 68(20): 2989-2991.

[13] Hong L, Xu J X. A chaotic crisis between chaotic saddle and attractor in forced Duffing oscillators. Communications in Nonlinear Science and Numerical Simulation, 2004, 9(3): 313-329.
[14] Tanaka G, Tsuji S, Aihara K. Grazing-induced crises in hybrid dynamical systems. Physics Letters A, 2009, 373(35): 3134-3139.
[15] Liu X, Hong L, Tang D, Yang L X. Crises in a fractional-order piecewise system. Nonlinear Dynamics, 2021, 103(3): 2855-2866.
[16] Borotto F A, Chian A C L, Hada T, Rempel E L. Chaos in driven Alfvén systems: boundary and interior crises. Physica D: Nonlinear Phenomena, 2004, 194(3-4): 275-282.
[17] Sommerer J C, Grebogi C. Determination of crisis parameter values by direct observation of manifold tangencies. International Journal of Bifurcation and Chaos, 1992, 2(2): 383-396.
[18] Grebogi C, Ott E, Yorke J A. Metamorphoses of basin boundaries in nonlinear dynamical systems. Physical Review Letters, 1986, 56(10): 1011-1014.
[19] Grebogi C, Ott E, Yorke J A. Basin boundary metamorphoses: changes in accessible boundary orbits. Nuclear Physics B-Proceedings Supplements, 1987, 2(C): 281-300.
[20] Osinga H M, Feudel U. Boundary crisis in quasiperiodically forced systems. Physica D: Nonlinear Phenomena, 2000, 141(1-2): 54-64.
[21] Gallas J A C, Grebogi C, Yorke J A. Vertices in parameter space: double crises which destroy chaotic attractors. Physical review letters, 1993, 71(9): 1359-1362.
[22] Stewart H B, Ueda Y, Grebogi C, Yorke J A. Double crises in two-parameter dynamical systems. Physical review letters, 1995, 75(13): 2478-2481.
[23] Osinga H M. Locus of boundary crisis: Expect infinitely many gaps. Physical Review E, 2006, 74(3): 035201.
[24] Tanaka G, Tsuji S, Aihara K. Grazing-induced crises in hybrid dynamical systems. Physics Letters A, 2009, 373(35): 3134-3139.
[25] Mason J F, Piiroinen P T. Interactions between global and grazing bifurcations in an impacting system. Chaos: An Interdisciplinary Journal of Nonlinear Science, 2011, 21(1):013113.
[26] De Freitas M S T, Viana R L, Grebogi C. Multistability, basin boundary structure, and chaotic behavior in a suspension bridge model. International Journal of Bifurcation and Chaos, 2004, 14(3): 927-950.
[27] Grebogi C, Ott E, Yorke J A. Critical exponent of chaotic transients in nonlinear dynamical systems. Physical review letters, 1986, 57(11): 1284-1287.
[28] Grebogi C, Ott E, Romeiras F, Yorke J A. Critical exponents for crisis-induced intermittency. Physical Review A, 1987, 36(11): 5365-5380.